Molecular Cell
Review

Proteasome Activators

Beth M. Stadtmueller[1] and Christopher P. Hill[1,*]
[1]Department of Biochemistry, University of Utah School of Medicine, Salt Lake City, UT 84112-5650, USA
*Correspondence: chris@biochem.utah.edu
DOI 10.1016/j.molcel.2010.12.020

Proteasomes degrade a multitude of protein substrates in the cytosol and nucleus, and thereby are essential for many aspects of cellular function. Because the proteolytic sites are sequestered in a closed barrel-shaped structure, activators are required to facilitate substrate access. Structural and biochemical studies of two activator families, 11S and Blm10, have provided insights to proteasome activation mechanisms, although the biological functions of these factors remain obscure. Recent advances have improved our understanding of the third activator family, including the 19S activator, which targets polyubiquitylated proteins for degradation. Here we present a structural perspective on how proteasomes are activated and how substrates are delivered to the proteolytic sites.

Introduction

Protein turnover is an essential and highly regulated process that is performed in cytosolic and nuclear compartments of eukaryotic cells primarily by proteasomes. This abundant protein complex is also found in archaea and in some eubacteria, and its activity is central to many cellular functions including protein quality control, DNA repair, transcription, cell-cycle regulation, signal transduction, and antigen presentation (Pickart and Cohen, 2004). "Proteasome" can refer to a variety of complexes whose cores comprise the cylindrical 20S proteasome (aka core particle/CP), which houses proteolytic sites within a central chamber. Because of this closed architecture, the 20S proteasome is an inherently repressed enzyme, although essentially any protein that enters the catalytic chamber will be degraded.

20S proteasomes are known to associate with three different families of activators that provide access to the central proteolytic chamber. The most broadly conserved family includes the eukaryotic 19S activator (aka regulatory particle/RP/PA700) and its archaeal PAN and eubacterial ARC/Mpa homologs. These factors require ATP hydrolysis to promote the degradation of protein substrates. The 19S activator, which can bind to one or both ends of a 20S proteasome to form a 26S proteasome, recognizes polyubiquitylated substrates, and may be comprised of multiple variants with distinct compositions and functions. The other two activator families are the 11S complexes (aka PA28, REG, PA26) and PA200/Blm10. These factors are less broadly conserved than the ATP-dependent activators, and their substrates and biological functions are less clear, although the mechanisms they use to activate proteasomes have been better characterized.

We begin by reviewing the architecture of the 20S proteasome, including features of the substrate entrance gate that maintain the default, closed conformations. We then discuss activation mechanisms, highlighting the insights provided by structures of proteasome-activator complexes. We compare and contrast the effects of activator binding on 20S proteasome structure and present a unified model for how activators open the entrance pore. Finally, we discuss models for how the ATP-dependent activators process substrates by unfolding and translocating them into the proteasome, and illustrate the emerging view that conformational changes make multiple contributions to 19S activator function.

The 20S Proteasome

Proteasomes comprise four stacked heptameric rings, two α type surrounding two β beta type, in an $\alpha_7\beta_7\beta_7\alpha_7$ pattern, to form a 28 subunit, barrel-like structure (Groll et al., 1997; Kwon et al., 2004; Lowe et al., 1995) (Figure 1A). The proteasome contains an interior chamber (Figure 1B), and the inner surface promotes protein unfolding (Ruschak et al., 2010). Although the α and β subunits share sequence and structural similarity, there are functionally important differences associated with their distinct N termini. The α subunit N-terminal residues form a gate at the center of the α ring that restricts substrate entry in the absence of an activator (Figure 1C) (Groll et al., 2000). The β subunit N termini contribute to the proteolytic active sites, which belong to the N-terminal nucleophile hydrolase family, and use a threonine side chain as the attacking nucleophile and the free N-terminal amine to activate an ordered water molecule that is incorporated into the product during hydrolysis (Figure 1D) (Brannigan et al., 1995; Seemuller et al., 1995). Archaea and eubacteria generally express just one α type and one β type subunit, resulting in proteasomes that have seven-fold symmetry. In contrast, eukaryotic proteasomes comprise seven distinct α subunits (α1–α7) and seven distinct β subunits (β1–β7) that each occupy unique positions in the respective rings, resulting in asymmetric structures with only approximate seven-fold symmetry. Just three of the seven eukaryotic β subunits, β1, β2, and β5, possess proteolytic sites, and these exhibit preference for cleavage following acidic, basic, or hydrophobic residues, respectively.

Higher eukaryotes express three additional catalytic β subunits (β1i, β2i, β5i) (Figure 1A), whose expression can be upregulated in interferon γ-inducible cells. These subunits replace their conventional counterparts to form immunoproteasomes that, consistent with optimal binding of peptides to MHC-I molecules, show reduced cleavage following acidic residues and enhanced cleavage following hydrophobic residues (Groettrup et al., 2010). Higher eukaryotes also encode a thymus-specific catalytic β subunit, β5t, which replaces β5 to form thymoproteasomes,

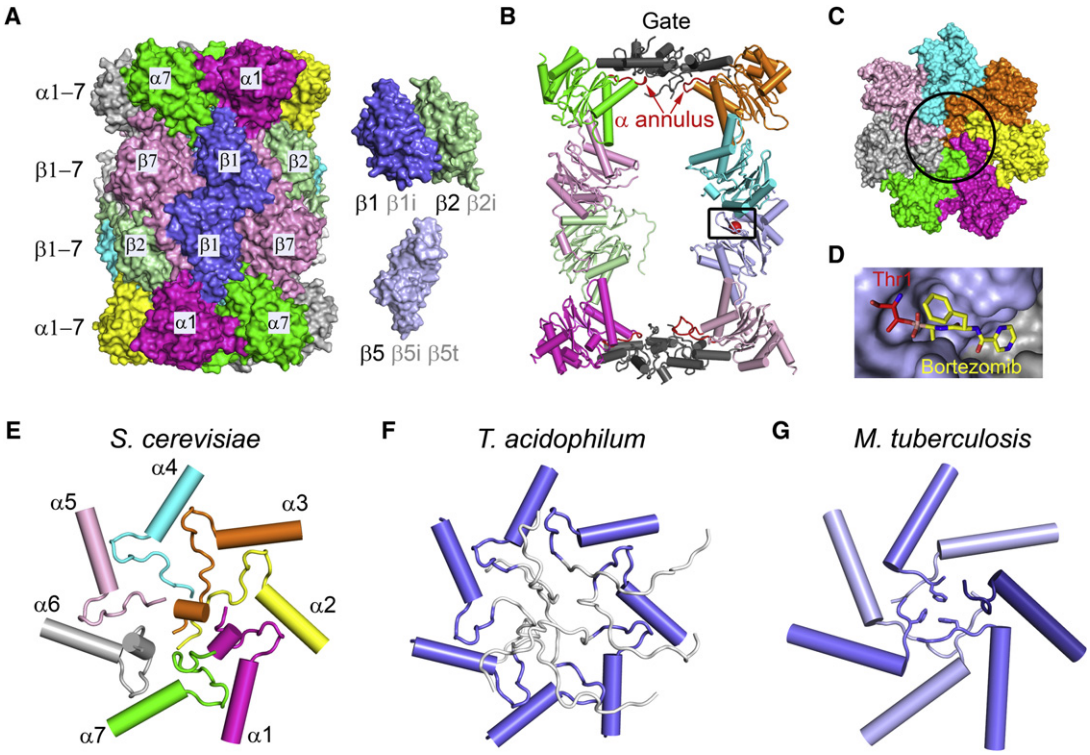

Figure 1. Structure of the 20S Proteasome

(A) Surface representation of the *S. cerevisiae* 20S proteasome (Groll et al., 1997). Individual subunits are labeled. β subunits shown to the right indicate that alternative counterparts can be expressed for some of the subunits. The bovine liver proteasome is closely superimposible to this structure (Unno et al., 2002). Archaeal and eubacterial 20S proteasomes are very similar but are typically comprised of one type of α and one type of β subunit, and are therefore seven-fold symmetric.

(B) Cutaway side view cartoon representation of the *S. cerevisiae* 20S proteasome. The region surrounding an active site is indicated with a box. The closed gate region is colored gray. The α annulus, just interior from the gate, is an opening formed by loops (red) in the α subunits.

(C) Top view surface representation of the *S. cerevisiae* 20S proteasome. The gate region is indicated with a circle.

(D) Close-up of the *S. cerevisiae* β5 active site in complex with the inhibitor bortezomib (Groll et al., 2006). Corresponds to the boxed region in (B).

(E) Top view cartoon of *S. cerevisiae* helix H0 and N-terminal residues that form the closed gate. This eukaryotic gate is sealed primarily by α2, α3, and α4, whose N-terminal residues are well ordered and participate in numerous hydrogen bonds and van der Waals contacts. Corresponds to the region circled in (C).

(F) Same as (E) for an archaeal gate (Religa et al., 2010). Residues shown in white are highly mobile.

(G) Same as (E) for a eubacterial gate (Li et al., 2010). This gate is ordered but is quite different from the eukaryotic structure. The seven subunits are chemically identical but adopt a total of three different conformations at their N termini, as indicated by the different shades. A phenylalanine side chain from each of the medium shade subunits contributes to the closed gate structure and is shown near the center of this panel.

which are thought to function in the positive selection of MHC class I restricted T cells because they have reduced ability to cleave after hydrophobic residues and thus produce peptides having weak affinity for MHC-I molecules (Murata et al., 2007).

Proteasomes can be valuable therapeutic targets. For example, bortezomib, a boronic acid peptide, inhibits the proteolytic sites by forming specific interactions between the boronate and the β subunit Thr1 side chain hydroxyl and main chain amine (Figure 1D). Bortezomib has high specificity for the human β5 proteolytic site and is used for the treatment of multiple myeloma and mantle cell lymphoma (Groll et al., 2009). Inhibitors targeting proteasome variants are also promising candidates for drug development, such as the recently described inhibitor PR-957, which specifically inhibits the β5i immunoproteasome subunit and shows promise for the treatment of autoimmune diseases (Muchamuel et al., 2009). Moreover, relatively large differences that exist between eukaryotic and eubacterial proteasome active sites offer the potential to develop antimicrobial drugs including those targeting *Mycobacterium tuberculosis* proteasomes (Lin et al., 2009).

The 20S Proteasome Gate

Substrates enter the proteasome through a gated pore in the center of each α subunit ring (Wenzel and Baumeister, 1995), and their passage is restricted by two structural elements. One obstacle is a narrow channel known as the α-annulus that is located slightly below the surface of the α ring (Figure 1B). Because this appears to be a fixed opening of 13 Å diameter (~20 Å in eubacteria), it ensures that substrates are substantially unfolded before they can enter the proteasome. The other obstacle is a closed gate formed from N-terminal residues of the α subunits, although the gate closure mechanism is different among bacteria, archaea, and eukarya. In eukaryotes, the closed gate adopts an ordered, asymmetric conformation that is defined by amino acid sequences that are unique to each α subunit (Figure 1E). This structure restricts entry of even small

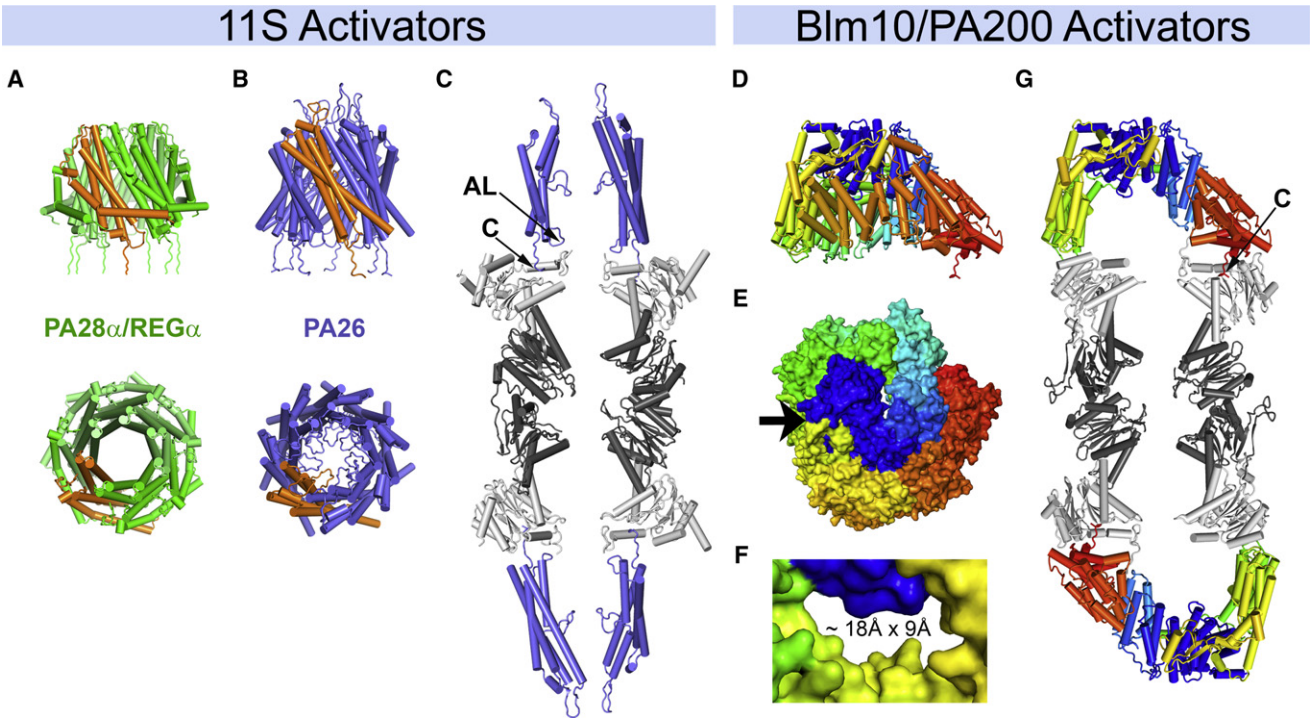

Figure 2. ATP-Independent Activators
(A) Side and top view cartoon representations of PA28α/REGα (Knowlton et al., 1997). A single subunit is colored orange.
(B) Same as (A) for PA26 as observed in proteasome complexes (Forster et al., 2005). Note the diaphragm-like structure formed in the central channel of PA26.
(C) Cutaway cartoon representation of the PA26-*S. cerevisiae* proteasome complex. This panel was generated by removing subunits, to leave a total of eight proteasome and four PA26 subunits. The PA26 activation loop (AL) and C terminus (C) are indicated for one of the subunits.
(D) Side view of Blm10 as seen in the proteasome complex (Sadre-Bazzaz et al., 2010). Rainbow colored, blue to red from N to C termini.
(E) Blm10 top view surface representation. An arrow indicates the largest opening through the Blm10 dome, which is not visible in this view.
(F) Close-up of the Blm10 pore viewed in the direction of the arrow in (E).
(G) Cutaway cartoon representation of the Blm10-proteasome complex. The Blm10 C terminus is indicated.

substrates; its importance is indicated by its precise conservation from yeast to mammals (Unno et al., 2002) and by the finding that a mutation disrupting this structure causes defects in the survival of yeast upon prolonged starvation (Bajorek et al., 2003). In contrast, while the 12 N-terminal residues of archaeal proteasome α subunits are also located at the entrance pore and can extend through the α-annulus to impede access of unfolded proteins, they are highly flexible (Benaroudj et al., 2003; Forster et al., 2003; Religa et al., 2010) (Figure 1F), thereby explaining why archaeal proteasomes display a relatively high level of activity toward small peptide substrates. It was initially thought that the eubacterial entrance pore resembled the unstructured archaeal gate, but recent structure determinations suggest instead that the N-terminal residues form a closed conformation that is ordered but nevertheless very different from that of eukaryotic proteasomes (Figure 1G) (Li et al., 2010).

11S Activators

Higher eukaryotes express three 11S isoforms called PA28α,β,γ (aka, REGα,β,γ) (Rechsteiner and Hill, 2005). PA28α and PA28β preferentially form a heteroheptamer, while PA28γ is a homoheptamer and appears to be the more ancient variant by virtue of its expression in most metazoans and in some single cell organisms, including *Dictyostelium discoideum* (Masson et al., 2009). The trypanosome *Trypanosoma brucei* expresses a homoheptameric 11S called PA26, whose sequence is highly divergent from the PA28 homologs but nevertheless retains the ability to activate proteasomes purified from a wide variety of species (Whitby et al., 2000). Although it is generally reported that 11S activators stimulate the hydrolysis of model peptide substrates but not proteins, REGγ/PA28γ has been implicated in the degradation of some natively unfolded proteins (Mao et al., 2008; Nie et al., 2010; Suzuki et al., 2009). Many studies have implicated PA28αβ in the production of MHC class I ligands, although the mechanistic basis for this function remains elusive (Groettrup et al., 2010).

Biochemical and structural studies of 11S activators are relatively advanced (Figure 2). The structure of human PA28α reveals elongated helical bundle subunits that assemble to form a heptameric ring that has a central channel 20–30 Å in diameter running along its length (Figure 2A) (Knowlton et al., 1997). The C-terminal residues of each subunit, which provide proteasome binding energy (Ma et al., 1993), and internal activation loops, which are critical for stimulation of peptide hydrolysis (Zhang et al., 1998), are arranged in a seven-fold symmetric array at the wide end of this torus-shaped molecule. The way in which these structural elements bind the proteasome and open the entrance pore was revealed by structures of PA26 in complex

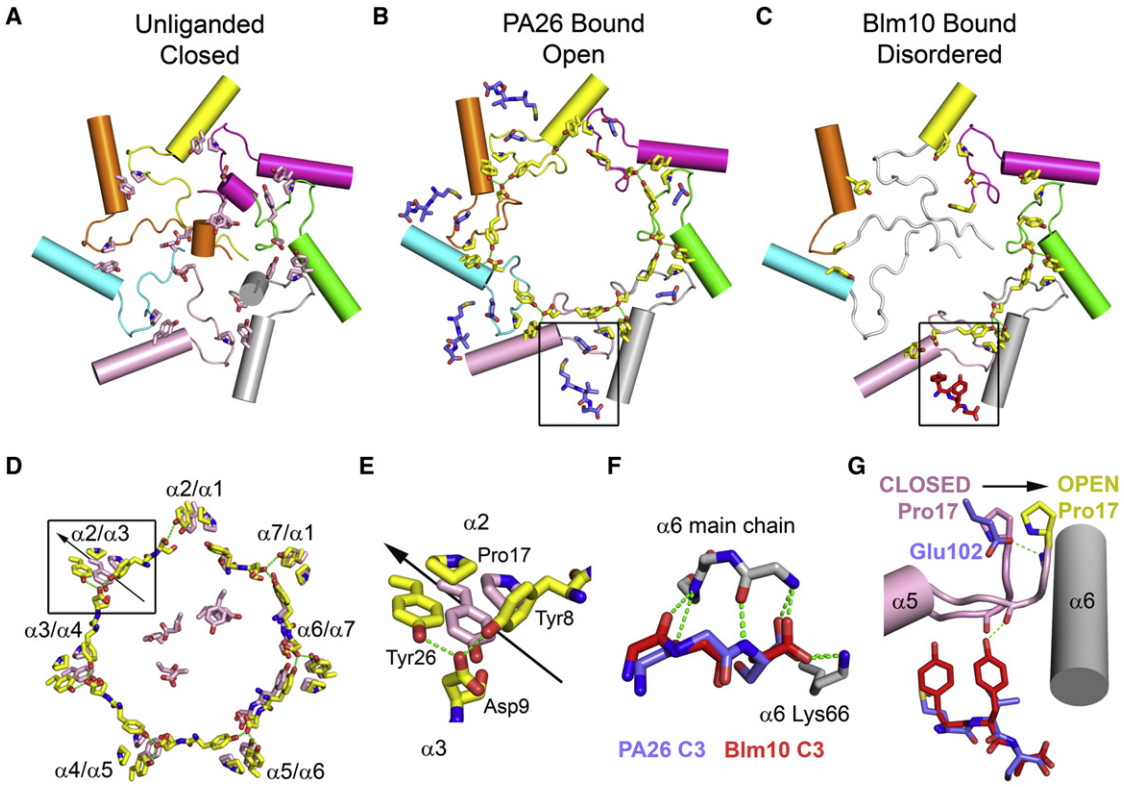

Figure 3. Mechanism of Gate Opening

(A) Top view of the *S. cerevisiae* proteasome gate in the closed conformation. Similar to Figure 1E but rotated and including the side chains of Tyr8, Asp9, Pro17, and Tyr26 (*T. acidophilum* numbering) of each subunit (pink). These residues stabilize the open conformation and in some cases also make interactions that stabilize the closed conformation shown here.

(B) Same as (A) for the PA26 complex, with Tyr8, Asp9, Pro17, and Tyr26 colored yellow. The C-terminal three residues of PA26 (blue) are shown in the four *S. cerevisiae* proteasome pockets where they are visible in the crystal structure (Forster et al., 2005). The pocket between α5 and α6 is boxed to encompass the PA26 C-terminal residues and also the Glu102 activation loop residue, which lies closer to the pseudo seven-fold axis and is shown for all seven PA26 subunits. The same open conformation is induced in an archaeal proteasome, when PA26 C-terminal residues bind equivalently to all seven pockets.

(C) Same as (B) for the Blm10 complex. Blm10 makes extensive contacts that completely surround the proteasome entrance pore (Figure 2G), and the C-terminal residues (red) bind in the α5/α6 pocket (boxed). In contrast to the PA26-bound structures, many N-terminal residues become disordered upon binding Blm10 (white, in the position of the unliganded structure).

(D) Superposition of the Tyr8, Asp9, Pro17, and Tyr26 residues of the open (yellow) and closed (pink) gate conformations following an alignment on the β subunits. This movement destabilizes packing in the closed conformation and widens the pore to allow a belt of Tyr8, Asp9 residues to assemble. The α2/α3 cluster, which undergoes the largest (3.5 Å) displacement of a Pro17 residue, is boxed, and the outward direction of displacement upon opening is indicated with an arrow.

(E) Close-up of the α2/α3 cluster boxed in (D).

(F) Close-up showing a subset of interactions that occur in the pocket boxed in (B) and (C) with PA26 and Blm10 C termini superimposed. Main-chain groups of PA26 and Blm10 C-terminal residues make equivalent hydrogen bonding interactions (dashed lines).

(G) Superposition of the PA26 and Blm10 complexes in the α5/α6 pocket illustrating the different mechanisms of displacing the Pro17 reverse turn. PA26 displaces Pro17 (in all seven subunits) by contacting adjacent residues with activation loop residue Glu102 (blue). Blm10 (red) stabilizes the same Pro17 displacement (just of α5) by forming a hydrogen bond (dashed lines) between its Tyr side chain and the main-chain oxygen of Gly19. ATPase activators likely use an equivalent penultimate Try interaction to induce gate opening.

with proteasomes from *S. cerevisiae* (Figures 2B and 2C) (Forster et al., 2003; Whitby et al., 2000) and *Thermoplasma acidophilum* (Forster et al., 2005).

As shown in Figure 3, PA26 C-terminal residues insert into pockets between proteasome α subunits where they form main-chain to main-chain hydrogen bonds and a salt bridge between the PA26 C-terminal carboxylate and a highly conserved proteasome lysine side chain (Lys 66) (Figures 3B and 3F). A glutamate side chain located in the PA26 activation loop contacts and repositions a conserved structural element located above the surface of the proteasome called the Pro17 reverse turn (Figure 3G). Small, 0.5–3.5 Å movements of each subunit's Pro17 reverse turn trigger gate opening by disrupting packing and hydrogen bonding interactions of the precisely closed conformation (Figure 3A) of eukaryotic proteasomes, and by widening the pore opening to a more circular arrangement that allows a belt of intersubunit contacts to form around the circumference of the opening (Figures 3D and 3E). Curiously, four α subunit residues that stabilize the open conformation in both the archaeal and yeast proteasome PA26 complex structures, Tyr8, Asp9, Pro17, and Tyr26 (Figures 3D and 3E), are highly conserved, even in species that do not express 11S activators. It was therefore postulated that this conservation exists because the same open proteasome conformation is

also induced by the ATP-dependent activators, which are found in essentially all species that express proteasomes. This idea was validated by biochemical analysis of mutant archaeal proteasomes and the ATPase activator PAN, which demonstrated that degradation of a model substrate protein is severely attenuated by mutation of Tyr8, Asp9, Pro17, or Tyr26 (Forster et al., 2003). Moreover, a similar argument that ATP-dependent activators use equivalent C-terminal interactions to those seen for PA26 was supported by the observation that the conserved lysine residue at the bottom of the pocket and the C-terminal residue of PAN subunits are both important for biochemical activity (Forster et al., 2005) and by electron microscopic reconstruction of proteasome complexes with peptides corresponding to the C terminus of PAN (Rabl et al., 2008).

While structural and biochemical studies on 11S have shed light on proteasome gate opening, an explanation for their physiological functions is less apparent. The central channel of PA28 might accommodate diffusion of small substrates and possibly even natively unstructured polypeptides. PA26, however, displays an insertion in helix 3 that projects into the central channel to form a diaphragm-like structure that is expected to impede passage of even peptide substrates (Figures 2B and 2C). The extent to which peptide diffusion is impeded is difficult to model, because the degree of flexibility is unclear. However, this structure prompts consideration of other explanations for the activation of proteasomes by 11S in biochemical assays, including the following: (1) 11S activators might leave the unliganded proteasome temporarily in an open conformation that can accept substrates after they dissociate, and (2) substrates might bind coincidently with the activator, perhaps located in the activator's central opening. The relevance of the biochemical activity for physiological function is also unclear, but one possibility is that they function in the context of hybrid proteasomes, in which they bind to the opposite end of the 20S proteasome from an 19S activator, and through as-yet-uncharacterized interactions localize the degradative capacity of the 19S activator complex to a specific cellular environment (Rechsteiner and Hill, 2005).

Blm10/PA200

Like 11S activators, Blm10/PA200 (*Saccharomyces cerevisiae*/human) does not utilize ATP and is generally believed to stimulate the hydrolysis of peptides but not proteins. Blm10/PA200 has been proposed to function in a surprisingly broad variety of processes, including 20S proteasome assembly (Fehlker et al., 2003), DNA repair (Schmidt et al., 2005; Ustrell et al., 2002), genomic stability (Blickwedehl et al., 2008), proteasome inhibition (Lehmann et al., 2008), spermatogenesis (Khor et al., 2006), and mitochondrial checkpoint regulation (Sadre-Bazzaz et al., 2010). This remarkable variety of functions may reflect the difficulty of identifying proximal action from a sea of indirect effects. Electron microscopic reconstructions of the PA200 and Blm10 proteasome complexes revealed similar dome-like architectures (Iwanczyk et al., 2006; Ortega et al., 2005; Schmidt et al., 2005). A recently reported yeast Blm10 20S crystal structure (Sadre-Bazzaz et al., 2010) revealed that Blm10 forms a HEAT repeat-like solenoid that makes 1.5 superhelical turns to form the dome that encloses a large (110,000 Å^3) volume and offers only a small (18 Å × 9 Å) opening through which substrates might pass (Figures 2D–2G). This closed architecture supports the proposal that Blm10/PA200 does not function in the degradation of proteins, and is consistent with the suggestion that Blm10/PA200 and 11S activators might serve as adaptors that function in the context of hybrid proteasomes. Further supporting the proposal that Blm10 is not a direct activator of proteolysis in vivo, it induces a proteasome gate structure that is disordered rather than fully open (Figure 3C). This structure is expected to allow passage of small peptides that can enter the opening through the dome, but, as with the disordered pore of the unliganded archaeal proteasome, it is not expected to allow passage of protein substrates. Thus, it is unclear how the gate conformation relates to Blm10/PA200 physiology beyond the requirement that it is an energetically accessible conformation that is compatible with binding.

Binding of Blm10 reveals an intriguing parallel with PA26 and, as discussed more fully in the following section, may provide insight into gate opening by the ATP-dependent activators. Of the many interactions in the large 10,000 Å^2 interface between Blm10 and the proteasome, contacts made by the Blm10 C terminus are especially notable. The three C-terminal residues insert into the pocket between α5 and α6 in a conformation that is superimposable with the PA26 C-terminal residues, including maintenance of the same hydrogen bonds between main-chain groups and the salt bridge between the activator C-terminal carboxylate and the conserved proteasome lysine side chain (Figure 3F). Unlike 11S activators such as PA26, but like ATPase subunits that function in gate opening (below), the penultimate residue of Blm10 is a tyrosine, or phenylalanine in some homologs. This tyrosine side chain contacts α5 Gly19 O to stabilize the α5 Pro17 reverse turn in the same position as seen in the open conformation with PA26 (Figure 3G). Thus, Blm10 couples binding of its C-terminal residues in the canonical 11S conformation to repositioning of a single subunit into the open conformation. This has the effect of moving the entire proteasome gate partially toward the fully open conformation seen with PA26, although the gate remains disordered rather than fully open because repositioning of α5 alone is insufficient to induce repositioning of all of the other α subunits, and because additional Blm10 contacts prevent the fully open conformation from forming (Sadre-Bazzaz et al., 2010).

Gate Opening by ATP-Dependent Activators

As noted above, evolutionary and biochemical evidence indicate that PAN, and presumably other ATP-dependent activators, utilize their C-terminal residues to bind 20S proteasomes in the same manner as PA26/11S and induce the same seven-fold symmetric open conformation. An important difference is that the penultimate tyrosine residue and a preceding hydrophobic residue found in the C termini of PAN subunits and in some of the 19S ATPase subunits can stimulate peptide degradation without employing an activation loop mechanism as observed for PA26/11S (Gillette et al., 2008; Smith et al., 2007).

How the PAN/19S C-terminal residues induce gate opening is somewhat controversial. One model, based on low-resolution structural studies, holds that binding induces closing of the binding pocket and a 4° rotation of the α subunits around the

α-annulus that subsequently induces gate opening (Rabl et al., 2008; Yu et al., 2010). A strength of this model is that it is based on electron microscopic observations of free complexes that are not restricted to a crystal lattice, although it does not provide a clear mechanism for how the conformational changes would be propagated. We favor an alternative model based on the crystal structure of the Blm10 complex (Sadre-Bazzaz et al., 2010) and on a series of chimeric PA26-proteasome complex crystal structures and binding studies (Stadtmueller et al., 2010). These structures verify that sequences corresponding to the PAN/19S C termini can bind superimposably with PA26 and Blm10 while using their penultimate tyrosine residue to contact and reposition the proteasome Pro17 reverse turn, thereby inducing the same open gate conformation as seen in the PA26 complex structures. These structures also reveal that a penultimate phenylalanine, which is conserved in PAN from many archaeal species, can stabilize the same repositioning of the Pro17 reverse turn, and surface plasmon resonance data indicate that a phenylalanine can contribute to activator binding affinity at a level similar to that of a penultimate tyrosine residue (Stadtmueller et al., 2010). This model relies heavily upon crystal structures, but its strengths include high-resolution structural information and a clear mechanism for how binding is coupled to gate opening. Another appealing aspect of this model is that it suggests a unified mechanism for gate opening in which all three types of activator make superimposable contacts through their C-terminal residues (Figure 3F) that provide binding affinity and dictate additional interactions that open the proteasome gate (Figure 3G). In the case of 11S activators, the activation loop provides gate-opening interactions, whereas the other activators use penultimate tyrosine or phenylalanine residues. Blm10 provides only one penultimate tyrosine interaction, which is not sufficient to fully open the gate, while the two or more penultimate tyrosine interactions of PAN/19S and the seven activation loop contacts of 11S result in complete gate opening.

Additional factors may contribute to mechanisms of gate opening by ATP-dependent activators. For example, ATP binding seems to be important (Liu et al., 2006; Smith et al., 2005), probably because ATP-induced conformational changes increase accessibility of C-terminal residues and hence binding. Binding of associated proteins or polyubiquitin to the 19S activator is also reported to promote gate opening (Bech-Otschir et al., 2009; Li and Demartino, 2009; Peth et al., 2009). These interactions could propagate conformational changes through the ATPase subunits to the 20S proteasome entrance pore, and/or they could influence substrate access through the pore in the center of the ring of ATPase subunits. Untangling these two possibilities remains a challenge.

A further consideration for gate opening is that a population of free 20S proteasome has been reported to exist in eukaryotic cells (Shibatani et al., 2006), and a substantial number of substrates are reportedly degraded by these proteasomes without the assistance of an activator (Baugh et al., 2009). Mechanisms associated with activator-independent degradation are poorly understood. One possibility is that thermal fluctuations induce spontaneous gate opening with some frequency, thereby allowing unstructured proteins to gain entry. Other possibilities are that specific peptides may stimulate gate opening (Kisselev et al., 2003) or that some substrates may contain binding determinants that induce formation of the open conformation, and thereby serve as their own activator for proteasome entry.

Although models for gate opening of eukaryotic and archaeal proteasomes are advanced, it is not clear how to think about eubacterial proteasomes in this regard. The lysine that is functionally important for binding 11S, Blm10, and PAN/19S appears to be conserved in the presumed activator binding pocket of eubacterial proteasomes, and eubacterial ARC/Mpa ATPases conserve the pentultimate tyrosine found in PAN and 19S subunits. These observations suggest that eubacterial proteasomes will bind their ATP-dependent ARC/Mpa activator in the same manner as their archaeal and eukaryotic cousins. On the other hand, eubacteria do not conserve the α subunit Tyr8, Asp9, Pro17, or Tyr26 residues that stabilize the open conformation in archaeal and eukaryotic 20S proteasomes. Thus, it will be of interest to determine the extent to which eubacterial proteasome gating parallels or diverges from the eukaryotic and archaeal mechanisms.

Substrate Unfolding and Translocation by ATP-Dependent Activators

The ATP-dependent proteasome activators are classical AAA ATPase family members (Erzberger and Berger, 2006) that actively unfold and translocate substrates. The archaeal/eubacterial PAN/ARC/Mpa activators are homohexameric ATPase rings, and the core of the eukaryotic 19S activator is a heterohexameric ATPase ring that is comprised of six different but related ATPase subunits (Rpt1-6) that each occupy a unique position within the ring (Tomko et al., 2010). The N-terminal and C-terminal regions of the six ATPases each interact to form two hexameric rings in the fully assembled complex. Binding studies and electron microscopy (Bohn et al., 2010; da Fonseca and Morris, 2008; Forster et al., 2010; Smith et al., 2005) have demonstrated that the C-terminal region, which includes the ATPase catalytic sites, is adjacent to the proteasome α ring, and the central pore of the ATPase subunit rings is roughly aligned with the proteasome entrance pore (Figure 4A).

Crystal structures have been reported for the N-terminal region of the *Rhodococcus erythropolis* ARC, *Archaeoglobus fulgidus* PAN (Djuranovic et al., 2009), *Methanocaldococcus jannaschii* PAN (Zhang et al., 2009a), and *Mycobacterium tuberculosis* Mpa (Wang et al., 2009, 2010). These reveal three dimeric coiled coils, formed by N-terminal residues from adjacent pairs of subunits, that are followed by a ring of OB domains (or tandem OB domains in eubacterial variants) to form a chalice-like hexamer with a central pore (Figures 4B and 4E). The striking mismatch between the trimeric arrangement of coiled-coil dimers and six-fold rotational symmetry of the OB regions (and presumably the ATPase domains) is accommodated by a conserved proline residue, Pro91 (*M. jannaschii* numbering), in the linker between the OB and coiled-coil domains. The conformation of the peptide bond preceding this residue alternates between *cis* and *trans* in subunits around the ring, with each coiled coil being formed by a Pro91 *cis-trans* pair of ATPase subunits. This model has been extended to the heteromeric ATPase hexamer at the heart of the 19S activator, where

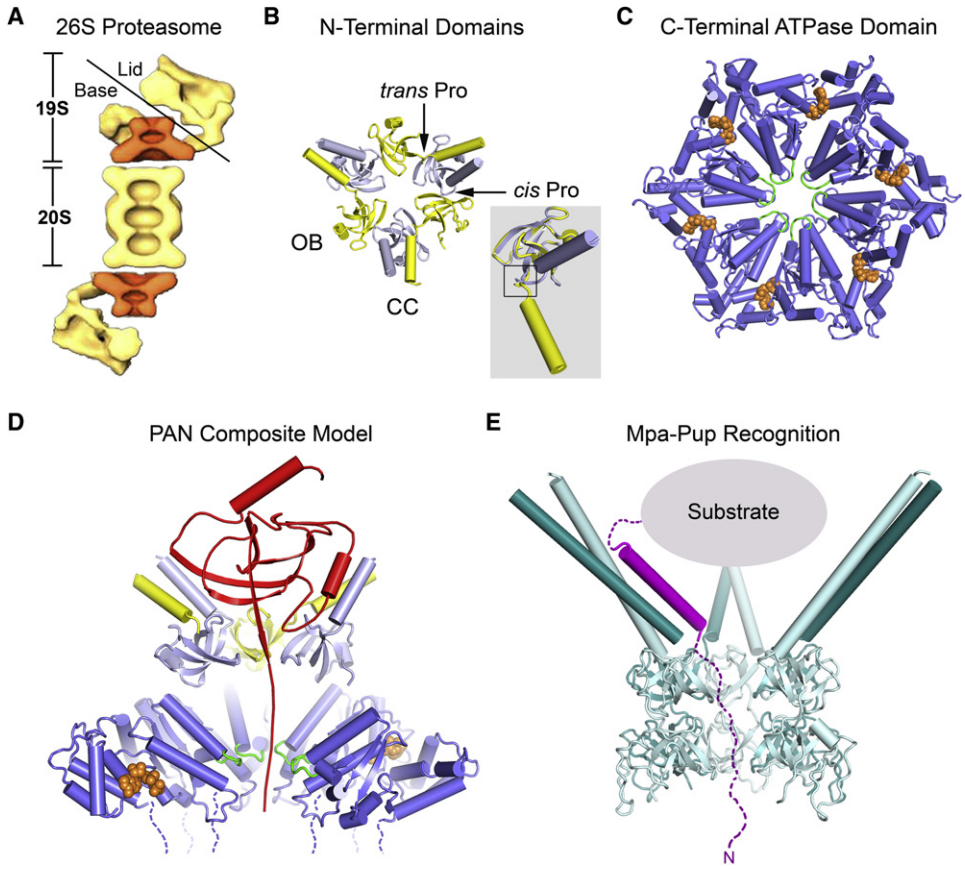

Figure 4. ATP-Dependent Activators

(A) Electron microscopic reconstruction of *Drosophila* 26S proteasome, adapted from Nickell et al. (2009) with permission. Lid and base subcomplexes of the 19S activator are indicated. The volume assigned to the ATPase subunits is colored orange.

(B) Top view of the N-terminal domains of PAN. The six subunits have identical sequences, but adopt alternating *cis*/*trans* conformations of Pro91 that allow formation of a trimer of coiled coils above a hexamer of OB domains. Inset shows a superposition of yellow (*trans*) and blue (*cis*) subunits on their OB domains to illustrate how the different conformations result in very different orientations for the N-terminal helix.

(C) Top view of the C-terminal ATPase domain of PAN. The monomer crystal structure was determined and is modeled here on the hexameric structure of HslU, following the approach of Zhang et al. (2009a). ATP/ADP sites are indicated in orange. Ar-Φ pore loop residues are colored green.

(D) Cutaway side view of a composite model of the PAN hexamer based on the available domain structures shown in (B) and (C). A substrate (red) is shown interacting with the N-terminal coiled coils, which promote protein unfolding, and with a flexible segment extending through the conduit of OB domains to reach the ATPase pore loops that drive translocation. PAN C termini (dashed lines) bind directly to 20S to induce gate opening.

(E) Model of *Mycobacterium tuberculosis* Pup-Mpa interactions based on crystal structures of Mpa N-terminal domains (Wang et al., 2010). Mpa displays a tandem OB domain, rather than the single OB domain of other ATPase activators. OB domains from a single Mpa subunit have been removed for clarity. Pup (purple) binds the Mpa coiled coil (teal) to present a disordered N-terminal segment (dashed line) that can traverse the OB domain conduit, with both Pup and conjugated substrate being subsequently dragged into the proteasome by the ATPase translocation activity. Binding stoichiometry and packing considerations suggest the arrangement shown here, with just one Pup-substrate associated with a Mpa hexamer.

Pro91 is conserved in Rpt2, Rpt3, and Rpt5, which appear to be the three subunits that require a *cis* proline configuration to accommodate the asymmetric structure (Zhang et al., 2009a). This finding is consistent with studies indicating that 19S assembles from precursor complexes containing the Rpt pairs Rpt1-Rpt2, Rpt6-Rpt3, and Rpt4-Rpt5 (Park et al., 2010), and targeted disulfide crosslinking studies of *S. cerevisiae* proteins demonstrate that Rpt subunits are ordered Rpt1-Rpt2-Rpt6-Rpt3-Rpt4-Rpt5 around the ring (Tomko et al., 2010).

A crystal structure has also been reported for the C-terminal ATPase domain of PAN from *Methanocaldococcus jannaschii* (Zhang et al., 2009a). Although this structure represents the monomeric, unassembled state, modeling based on the bacterial ATPase HslU (Bochtler et al., 2000; Sousa et al., 2000) indicates that the ATPase domain forms a ring with a central pore that displays an Ar-Φ loop (aka pore loop 1) from each of the six subunits (Figure 4C) (Zhang et al., 2009a). AR-Φ loops are conserved among ATPase domains of AAA ATPase such as HslU and are thought to move upon ATP hydrolysis to drive substrate translocation (Park et al., 2005). Thus, the PAN Ar-Φ loop (Phe244-Ile245-Gly246) likely paddles substrates through the pore, with a leading role being played by the aromatic Phe244 side chain and the Gly246 being required to allow the conformational changes to occur (Zhang et al., 2009b). Genetic analysis in *S. cerevisiae* demonstrated that mutation of the equivalent residues in 19S Rpt subunits led to proteolysis

defects (Zhang et al., 2009b), which further supports the model that PAN and 19S ATPases adopt equivalent structures and mechanisms. The paddling model accounts for how "simple" sequences (Tian et al., 2005), that are thought to interact weakly with the pore loops, allow adjacent, stable domains to escape degradation, as reported for a number of transcription factors that use this mechanism to release active signaling domains that relocate to the nucleus (Rape and Jentsch, 2004). An important, outstanding mechanistic question is how movements of the pore loops in a hexamer are coordinated to promote substrate translocation. Indeed, extensive studies on other AAA ATPases have provided support for a variety of models, including sequential action of each subunit (Enemark and Joshua-Tor, 2006; Thomsen and Berger, 2009), stochastic/probabilistic firing of individual subunits (Martin et al., 2005), and concerted movement of all pore loops (Gai et al., 2004).

A composite PAN model proposes that the coiled coils sit above a conduit of OB domains through which substrates pass before engaging the translocating pore loops of the ATPase domains (Zhang et al., 2009a) (Figure 4D). The corresponding Rpt assembly has been localized in the 19S activator (Bohn et al., 2010) (Figure 4A), and the structure of an N-terminal region of *Mycobacterium* Mpa supports an analogous model for eubacterial activators (Wang et al., 2010) (Figure 4E). This model explains why proteasome substrates must include a flexible segment, which can be an internal loop, in order to be processed, because only an unstructured sequence could reach from the top surface to engage the ATPase pore loops and initiate translocation (Prakash et al., 2004, 2009). Although substrate translocation promotes unfolding by forcing the substrate through a narrow channel, ATP-independent mechanisms also contribute to the functions of ATP-dependent activators. The N-terminal coiled coils structurally resemble the chaperone prefoldin and, by virtue of their overall structure, can promote protein unfolding (Djuranovic et al., 2009). It also appears that unfolding on the ATPase surface can be promoted by nucleotide binding and hydrolysis, although the mechanism of coupling between the N- and C-terminal regions of the ATPase subunits is currently unclear (Zhang et al., 2009b).

Substrate Targeting to ATP-Dependent Activators

Proteasome ATP-dependent activator function is coupled to cellular substrate targeting strategies. Substrates must include both a flexible sequence that can reach the ATPase pore loops and affinity for the ATPase that may be either inherent or provided by posttranslational modification. The eubacterium *Mycobacterium tuberculosis* targets substrates to Mpa using Pup (prokaryotic ubiquitin-like protein), which is a natively unstructured protein that when conjugated to a substrate provides both affinity for the ATPases and a means to engage the pore loops. In contrast to ubiquitin, which is typically removed prior to degradation of the substrate, Pup is translocated and degraded together with the substrate (Burns et al., 2010; Pearce et al., 2008; Striebel et al., 2010), a targeting strategy that may explain why the eubacterial α-annulus is wider than that of eukaryotic (or archaeal) proteasomes. An attractive model for how Pup delivers substrates to the Mpa activator and on to the eubacterial 20S proteasome is provided by crystal structures of Mpa and Pup complexes (Wang et al., 2010), which indicate that Pup binding to Mpa coiled coils induces the formation of a Pup helix that positions the flexible Pup N terminus for engagement with the pore loops (Figure 4E). The archaeal SAMP1/2 proteins appear to play proteasome-targeting roles analogous to those of Pup and ubiquitin, although mechanistic details are less clear (Humbard et al., 2010).

Whereas the archaeal and eubacterial ATPase activators appear to be autonomous complexes that can process substrates without the assistance of additional factors, the eukaryotic 19S activator is generally estimated to comprise 19 different stoichiometric subunits including the six ATPases. This considerably expanded complexity appears to provide an interface with the eukaryotic targeting pathways, the most prominent of which involve ubiquitylation (Finley, 2009). Hundreds of human proteins are thought to function in ubiquitylation and deubiquitylation pathways, some of which are 19S subunits. Several of the 19S non-ATPase subunits can recognize ubiquitin conjugated proteins, and some are enzymes that can edit the chain (extend/trim) to alter substrate affinity for 19S or remove polyubiquitin chains as the ATPases translocate the substrate into the proteasome. This process can be further regulated by many tens of additional proteins that have been characterized as substoichiometric 19S subunits that presumably associate with the core machinery and tailor its activity to specific physiological contexts (Finley, 2009).

19S Structure and Dynamics

The challenging task of obtaining structural information on the 19S activator is a topic of intense effort and debate. An attractive composite model, provided by electron microscopic and informatics analysis (Bohn et al., 2010; Forster et al., 2010), places the ATPases adjacent to the 20S proteasome (Figure 4A). In this model, 19S subunits form two major subassemblies, the base and the lid (Glickman et al., 1998). The base includes the six Rpt ATPases, two scaffolding proteins (Rpn1-2) and several proteins (Rpn10, Rpn13, and Uch37) involved in ubiquitin recognition and processing, whereas the lid contains at least one deubiquitylating enzyme, Rpn11, and eight other proteins (Rpn3,5-9,12,15) whose individual functions are uncharacterized. An alternative model suggests that the Rpn1 and Rpn2 scaffolding proteins form a tower above the 20S proteasome entrance pore (Rosenzweig et al., 2008), although, as discussed above, the model in which the ATPase ring occupies this position is generally preferred (Forster et al., 2010; Tomko et al., 2010). Another controversial proposal is that 26S proteasome assembly and disassembly are integral to the mechanism of protein degradation (Babbitt et al., 2005), although the generally preferred view is that 26S proteasomes catalyze multiple rounds of degradation without disassembly (Kriegenburg et al., 2008).

In addition to a need for high-resolution structural data, understanding 19S mechanisms will require unraveling the functional consequences of subunit conformational changes beyond those already inferred for the ATPase pore loops. For example, shuttle receptors such as Rad23, which can bind both polyubiquitin and 19S, are comprised of a ubiquitin-like (Ubl) domain and ubiquitin-associated (UBA) domains. These domains associate with each other in the absence of substrate, but upon binding of

polyubiquitin to the UBA domains the Ubl domain is liberated to associate with its receptor on 19S (Walters et al., 2003). The Ubp6/USP14 and Uch37 deubiquitylating enzymes are also activated upon binding to 19S, although the mechanisms and associated conformational changes are not currently well understood (Lam et al., 1997; Leggett et al., 2002). Moreover, Uch37's binding partner, the ubiquitin receptor Rpn13 (Yao et al., 2006), undergoes a functionally important conformational change upon binding the 19S Rpn2 subunit, whereupon its ubiquitin-binding activity is increased 26-fold (Chen et al., 2010).

A dramatic example illustrating how conformational changes contribute to 19S function is provided by the 19S lid subunit Rpn11/POH1 (*S. cerevisiae*/human), which is a deubiquitylating enzyme that removes ubiquitin chains en bloc in order to facilitate entry of substrate to the proteasome and to avoid depleting pools of free ubiquitin (Verma et al., 2002; Yao and Cohen, 2002). Ubiquitin has seven lysine residues, each of which can be used to build a polyubiquitin chain, with all types of chain linkage except Lys63 serving as efficient tags for proteasomal degradation (Xu et al., 2009). Interestingly, POH1 preferentially cleaves Lys63 isopeptide bonds (Cooper et al., 2009), which suggests that it rapidly disassembles Lys63 chains in an ATP-independent manner in order to spare mistargeted substrates from degradation. Paradoxically, authentic proteasome substrates are poor Rpn11/POH substrates, and their processing requires ATP hydrolysis by the Rpt subunits. This indicates that the ATPases drive the substrate into a productive conformation in the Rpn11/POH1 active site, and ensures that substrates engage the ATPases before the chain is removed. This is an effective strategy to ensure that substrates are translocated and are not released prior to degradation (Cooper et al., 2009). The coupling between ATPases in the 19S base and a deubiquitylating enzyme in the 19S lid indicates that conformational changes coordinated throughout the 900kDa complex are functionally important.

Concluding Remarks

Currently we understand many fundamental aspects of proteasome function and mechanism. We know the structure of the 20S proteasome and of many inhibitor complexes at high resolution and have a detailed model of the catalytic mechanism. We also understand that substrates enter through an axial pore that is gated by activators. Detailed structural models are available for proteasome complexes with the 11S and Blm10 activators, and emerging models describe how ATP-dependent activators induce gate opening. We also have an approximate model for how the ATP-dependent activators promote substrate unfolding and translocation, and we are beginning to understand other details of 19S mechanism, including high-resolution structures of some subunits and models describing functionally important conformational changes.

Despite these advances, many unknowns cloud our understanding of proteasome function. We do not have a firm grasp on the biological roles played by 11S and Blm10/PA200 activators, or the relevance of hybrid proteasomes. We lack atomic structures of most 19S components and, more importantly, we do not fully understand how these components interact with each other and move during their functional cycle. Uncertainty even exists regarding 19S composition and the designation of some subunits as being stoichiometric or substoichimetric, and considerable uncertainty exists regarding the functional relevance of the many substoichiometric subunits that have been reported. The recognition that all three classes of activators use their C-terminal residues to bind 20S in the same manner, and the finding that some C-terminal tripeptide sequences have higher affinity and can trigger gate opening, suggests that currently unrecognized proteins may use the same principles to bind, and possibly activate, the proteasome. While it is clear that coordinated conformational changes are an important aspect of 19S function, the possibility of an allosteric relationship between 19S and the 20S proteolytic sites, which are at least 60 Å distant, is unclear. Although some reports indicate that such an allosteric relationship exists (Kisselev et al., 2003; Kleijnen et al., 2007; Li et al., 2001; Osmulski et al., 2009) as yet no direct visualization of relevant conformational changes has been described.

In a general sense, much more remains to be learned about the regulation of proteasome activity, as indicated by the recent finding that the 19S subunit Rpn10 is itself ubiquitylated in order to inhibit its ubiquitin-binding activity and to target it for proteasomal degradation (Isasa et al., 2010), and the finding that an inhibitor of the proteasome-associated USP14 deubiquitylating enzyme can enhance 26S proteolytic function (Lee et al., 2010). Finally, an important area of research that we have not discussed is the assembly pathways of 20S and 26S proteasomes, where rapid progress is being made but major questions, such as a possible role of the 20S proteasome in promoting 19S assembly, are still outstanding (Murata et al., 2009; Park et al., 2010). Overall, these challenges invite future efforts to better define functions of protein complexes that stably interact with the proteasome, and the mechanisms by which they regulate substrate degradation.

ACKNOWLEDGMENTS

We thank Robert Cohen, Martin Rechsteiner, Tim Formosa, and members of the Hill lab for critical comments on the manuscript. Figures were made using Pymol (DeLano, 2002). Our work on proteasomes is supported by National Institutes of Health GM59135.

REFERENCES

Babbitt, S.E., Kiss, A., Deffenbaugh, A.E., Chang, Y.H., Bailly, E., Erdjument-Bromage, H., Tempst, P., Buranda, T., Sklar, L.A., Baumler, J., et al. (2005). ATP hydrolysis-dependent disassembly of the 26S proteasome is part of the catalytic cycle. Cell *121*, 553–565.

Bajorek, M., Finley, D., and Glickman, M.H. (2003). Proteasome disassembly and downregulation is correlated with viability during stationary phase. Curr. Biol. *13*, 1140–1144.

Baugh, J.M., Viktorova, E.G., and Pilipenko, E.V. (2009). Proteasomes can degrade a significant proportion of cellular proteins independent of ubiquitination. J. Mol. Biol. *386*, 814–827.

Bech-Otschir, D., Helfrich, A., Enenkel, C., Consiglieri, G., Seeger, M., Holzhutter, H.G., Dahlmann, B., and Kloetzel, P.M. (2009). Polyubiquitin substrates allosterically activate their own degradation by the 26S proteasome. Nat. Struct. Mol. Biol. *16*, 219–225.

Benaroudj, N., Zwickl, P., Seemuller, E., Baumeister, W., and Goldberg, A.L. (2003). ATP hydrolysis by the proteasome regulatory complex PAN serves multiple functions in protein degradation. Mol. Cell *11*, 69–78.

Blickwedehl, J., Agarwal, M., Seong, C., Pandita, R.K., Melendy, T., Sung, P., Pandita, T.K., and Bangia, N. (2008). Role for proteasome activator PA200 and postglutamyl proteasome activity in genomic stability. Proc. Natl. Acad. Sci. USA *105*, 16165–16170.

Bochtler, M., Hartmann, C., Song, H.K., Bourenkov, G.P., Bartunik, H.D., and Huber, R. (2000). The structures of HsIU and the ATP-dependent protease HsIU-HsIV. Nature *403*, 800–805.

Bohn, S., Beck, F., Sakata, E., Walzthoeni, T., Beck, M., Aebersold, R., Forster, F., Baumeister, W., and Nickell, S. (2010). From the cover: structure of the 26S proteasome from Schizosaccharomyces pombe at subnanometer resolution. Proc. Natl. Acad. Sci. USA *107*, 20992–20997.

Brannigan, J.A., Dodson, G., Duggleby, H.J., Moody, P.C., Smith, J.L., Tomchick, D.R., and Murzin, A.G. (1995). A protein catalytic framework with an N-terminal nucleophile is capable of self-activation. Nature *378*, 416–419.

Burns, K.E., Pearce, M.J., and Darwin, K.H. (2010). Prokaryotic ubiquitin-like protein provides a two-part degron to Mycobacterium proteasome substrates. J. Bacteriol. *192*, 2933–2935.

Chen, X., Lee, B.H., Finley, D., and Walters, K.J. (2010). Structure of proteasome ubiquitin receptor hRpn13 and its activation by the scaffolding protein hRpn2. Mol. Cell *38*, 404–415.

Cooper, E.M., Cutcliffe, C., Kristiansen, T.Z., Pandey, A., Pickart, C.M., and Cohen, R.E. (2009). K63-specific deubiquitination by two JAMM/MPN+ complexes: BRISC-associated Brcc36 and proteasomal Poh1. EMBO J. *28*, 621–631.

da Fonseca, P.C., and Morris, E.P. (2008). Structure of the human 26S proteasome: subunit radial displacements open the gate into the proteolytic core. J. Biol. Chem. *283*, 23305–23314.

DeLano, W.L. (2002). The PyMOL Molecular Graphics System (San Carlos, CA:: DeLano Scientific).

Djuranovic, S., Hartmann, M.D., Habeck, M., Ursinus, A., Zwickl, P., Martin, J., Lupas, A.N., and Zeth, K. (2009). Structure and activity of the N-terminal substrate recognition domains in proteasomal ATPases. Mol. Cell *34*, 580–590.

Enemark, E.J., and Joshua-Tor, L. (2006). Mechanism of DNA translocation in a replicative hexameric helicase. Nature *442*, 270–275.

Erzberger, J.P., and Berger, J.M. (2006). Evolutionary relationships and structural mechanisms of AAA+ proteins. Annu. Rev. Biophys. Biomol. Struct. *35*, 93–114.

Fehlker, M., Wendler, P., Lehmann, A., and Enenkel, C. (2003). Blm3 is part of nascent proteasomes and is involved in a late stage of nuclear proteasome assembly. EMBO Rep. *4*, 959–963.

Finley, D. (2009). Recognition and processing of ubiquitin-protein conjugates by the proteasome. Annu. Rev. Biochem. *78*, 477–513.

Forster, A., Whitby, F.G., and Hill, C.P. (2003). The pore of activated 20S proteasomes has an ordered 7-fold symmetric conformation. EMBO J. *22*, 4356–4364.

Forster, A., Masters, E.I., Whitby, F.G., Robinson, H., and Hill, C.P. (2005). The 1.9 Å structure of a proteasome-11S activator complex and implications for proteasome-PAN/PA700 interactions. Mol. Cell *18*, 589–599.

Forster, F., Lasker, K., Nickell, S., Sali, A., and Baumeister, W. (2010). Towards an integrated structural model of the 26S proteasome. Mol. Cell. Proteomics *9*, 1666–1677.

Gai, D., Zhao, R., Li, D., Finkielstein, C.V., and Chen, X.S. (2004). Mechanisms of conformational change for a replicative hexameric helicase of SV40 large tumor antigen. Cell *119*, 47–60.

Gillette, T.G., Kumar, B., Thompson, D., Slaughter, C.A., and DeMartino, G.N. (2008). Differential roles of the COOH termini of AAA subunits of PA700 (19 S regulator) in asymmetric assembly and activation of the 26 S proteasome. J. Biol. Chem. *283*, 31813–31822.

Glickman, M.H., Rubin, D.M., Coux, O., Wefes, I., Pfeifer, G., Cjeka, Z., Baumeister, W., Fried, V.A., and Finley, D. (1998). A subcomplex of the proteasome regulatory particle required for ubiquitin-conjugate degradation and related to the COP9-signalosome and eIF3. Cell *94*, 615–623.

Groettrup, M., Kirk, C.J., and Basler, M. (2010). Proteasomes in immune cells: more than peptide producers? Nat. Rev. Immunol. *10*, 73–78.

Groll, M., Ditzel, L., Lowe, J., Stock, D., Bochtler, M., Bartunik, H.D., and Huber, R. (1997). Structure of 20S proteasome from yeast at 2.4 Å resolution. Nature *386*, 463–471.

Groll, M., Bajorek, M., Kohler, A., Moroder, L., Rubin, D.M., Huber, R., Glickman, M.H., and Finley, D. (2000). A gated channel into the proteasome core particle. Nat. Struct. Biol. *7*, 1062–1067.

Groll, M., Berkers, C.R., Ploegh, H.L., and Ovaa, H. (2006). Crystal structure of the boronic acid-based proteasome inhibitor bortezomib in complex with the yeast 20S proteasome. Structure *14*, 451–456.

Groll, M., Huber, R., and Moroder, L. (2009). The persisting challenge of selective and specific proteasome inhibition. J. Pept. Sci. *15*, 58–66.

Humbard, M.A., Miranda, H.V., Lim, J.M., Krause, D.J., Pritz, J.R., Zhou, G., Chen, S., Wells, L., and Maupin-Furlow, J.A. (2010). Ubiquitin-like small archaeal modifier proteins (SAMPs) in Haloferax volcanii. Nature *463*, 54–60.

Isasa, M., Katz, E.J., Kim, W., Yugo, V., Gonzalez, S., Kirkpatrick, D.S., Thomson, T.M., Finley, D., Gygi, S.P., and Crosas, B. (2010). Monoubiquitination of RPN10 regulates substrate recruitment to the proteasome. Mol. Cell *38*, 733–745.

Iwanczyk, J., Sadre-Bazzaz, K., Ferrell, K., Kondrashkina, E., Formosa, T., Hill, C.P., and Ortega, J. (2006). Structure of the Blm10-20 S proteasome complex by cryo-electron microscopy. Insights into the mechanism of activation of mature yeast proteasomes. J. Mol. Biol. *363*, 648–659.

Khor, B., Bredemeyer, A.L., Huang, C.Y., Turnbull, I.R., Evans, R., Maggi, L.B., Jr., White, J.M., Walker, L.M., Carnes, K., Hess, R.A., and Sleckman, B.P. (2006). Proteasome activator PA200 is required for normal spermatogenesis. Mol. Cell. Biol. *26*, 2999–3007.

Kisselev, A.F., Garcia-Calvo, M., Overkleeft, H.S., Peterson, E., Pennington, M.W., Ploegh, H.L., Thornberry, N.A., and Goldberg, A.L. (2003). The caspase-like sites of proteasomes, their substrate specificity, new inhibitors and substrates, and allosteric interactions with the trypsin-like sites. J. Biol. Chem. *278*, 35869–35877.

Kleijnen, M.F., Roelofs, J., Park, S., Hathaway, N.A., Glickman, M., King, R.W., and Finley, D. (2007). Stability of the proteasome can be regulated allosterically through engagement of its proteolytic active sites. Nat. Struct. Mol. Biol. *14*, 1180–1188.

Knowlton, J.R., Johnston, S.C., Whitby, F.G., Realini, C., Zhang, Z., Rechsteiner, M., and Hill, C.P. (1997). Structure of the proteasome activator REGalpha (PA28alpha). Nature *390*, 639–643.

Kriegenburg, F., Seeger, M., Saeki, Y., Tanaka, K., Lauridsen, A.M., Hartmann-Petersen, R., and Hendil, K.B. (2008). Mammalian 26S proteasomes remain intact during protein degradation. Cell *135*, 355–365.

Kwon, Y.D., Nagy, I., Adams, P.D., Baumeister, W., and Jap, B.K. (2004). Crystal structures of the Rhodococcus proteasome with and without its pro-peptides: implications for the role of the pro-peptide in proteasome assembly. J. Mol. Biol. *335*, 233–245.

Lam, Y.A., DeMartino, G.N., Pickart, C.M., and Cohen, R.E. (1997). Specificity of the ubiquitin isopeptidase in the PA700 regulatory complex of 26 S proteasomes. J. Biol. Chem. *272*, 28438–28446.

Lee, B.H., Lee, M.J., Park, S., Oh, D.C., Elsasser, S., Chen, P.C., Gartner, C., Dimova, N., Hanna, J., Gygi, S.P., et al. (2010). Enhancement of proteasome activity by a small-molecule inhibitor of USP14. Nature *467*, 179–184.

Leggett, D.S., Hanna, J., Borodovsky, A., Crosas, B., Schmidt, M., Baker, R.T., Walz, T., Ploegh, H., and Finley, D. (2002). Multiple associated proteins regulate proteasome structure and function. Mol. Cell *10*, 495–507.

Lehmann, A., Jechow, K., and Enenkel, C. (2008). Blm10 binds to pre-activated proteasome core particles with open gate conformation. EMBO Rep. *9*, 1237–1243.

Li, X., and Demartino, G.N. (2009). Variably modulated gating of the 26S proteasome by ATP and polyubiquitin. Biochem. J. *421*, 397–404.

Li, J., Gao, X., Ortega, J., Nazif, T., Joss, L., Bogyo, M., Steven, A.C., and Rechsteiner, M. (2001). Lysine 188 substitutions convert the pattern of proteasome activation by REGgamma to that of REGs alpha and beta. EMBO J. *20*, 3359–3369.

Li, D., Li, H., Wang, T., Pan, H., and Lin, G. (2010). Structural basis for the assembly and gate closure mechanisms of the Mycobacterium tuberculosis 20S proteasome. EMBO J. *29*, 2037–2047.

Lin, G., Li, D., de Carvalho, L.P., Deng, H., Tao, H., Vogt, G., Wu, K., Schneider, J., Chidawanyika, T., Warren, J.D., et al. (2009). Inhibitors selective for mycobacterial versus human proteasomes. Nature *461*, 621–626.

Liu, C.W., Li, X., Thompson, D., Wooding, K., Chang, T.L., Tang, Z., Yu, H., Thomas, P.J., and DeMartino, G.N. (2006). ATP binding and ATP hydrolysis play distinct roles in the function of 26S proteasome. Mol. Cell *24*, 39–50.

Lowe, J., Stock, D., Jap, B., Zwickl, P., Baumeister, W., and Huber, R. (1995). Crystal structure of the 20S proteasome from the archaeon T. acidophilum at 3.4 Å resolution. Science *268*, 533–539.

Ma, C.P., Willy, P.J., Slaughter, C.A., and DeMartino, G.N. (1993). PA28, an activator of the 20 S proteasome, is inactivated by proteolytic modification at its carboxyl terminus. J. Biol. Chem. *268*, 22514–22519.

Mao, I., Liu, J., Li, X., and Luo, H. (2008). REGgamma, a proteasome activator and beyond? Cell. Mol. Life Sci. *65*, 3971–3980.

Martin, A., Baker, T.A., and Sauer, R.T. (2005). Rebuilt AAA + motors reveal operating principles for ATP-fuelled machines. Nature *437*, 1115–1120.

Masson, P., Lundin, D., Soderbom, F., and Young, P. (2009). Characterization of a REG/PA28 proteasome activator homolog in Dictyostelium discoideum indicates that the ubiquitin- and ATP-independent REGgamma proteasome is an ancient nuclear protease. Eukaryot. Cell *8*, 844–851.

Muchamuel, T., Basler, M., Aujay, M.A., Suzuki, E., Kalim, K.W., Lauer, C., Sylvain, C., Ring, E.R., Shields, J., Jiang, J., et al. (2009). A selective inhibitor of the immunoproteasome subunit LMP7 blocks cytokine production and attenuates progression of experimental arthritis. Nat. Med. *15*, 781–787.

Murata, S., Sasaki, K., Kishimoto, T., Niwa, S., Hayashi, H., Takahama, Y., and Tanaka, K. (2007). Regulation of CD8+ T cell development by thymus-specific proteasomes. Science *316*, 1349–1353.

Murata, S., Yashiroda, H., and Tanaka, K. (2009). Molecular mechanisms of proteasome assembly. Nat. Rev. Mol. Cell Biol. *10*, 104–115.

Nickell, S., Beck, F., Scheres, S.H., Korinek, A., Forster, F., Lasker, K., Mihalache, O., Sun, N., Nagy, I., Sali, A., et al. (2009). Insights into the molecular architecture of the 26S proteasome. Proc. Natl. Acad. Sci. USA *106*, 11943–11947.

Nie, J., Wu, M., Wang, J., Xing, G., He, F., and Zhang, L. (2010). REGgamma proteasome mediates degradation of the ubiquitin ligase Smurf1. FEBS Lett. *584*, 3021–3027.

Ortega, J., Heymann, J.B., Kajava, A.V., Ustrell, V., Rechsteiner, M., and Steven, A.C. (2005). The axial channel of the 20S proteasome opens upon binding of the PA200 activator. J. Mol. Biol. *346*, 1221–1227.

Osmulski, P.A., Hochstrasser, M., and Gaczynska, M. (2009). A tetrahedral transition state at the active sites of the 20S proteasome is coupled to opening of the alpha-ring channel. Structure *17*, 1137–1147.

Park, E., Rho, Y.M., Koh, O.J., Ahn, S.W., Seong, I.S., Song, J.J., Bang, O., Seol, J.H., Wang, J., Eom, S.H., and Chung, C.H. (2005). Role of the GYVG pore motif of HslU ATPase in protein unfolding and translocation for degradation by HslV peptidase. J. Biol. Chem. *280*, 22892–22898.

Park, S., Tian, G., Roelofs, J., and Finley, D. (2010). Assembly manual for the proteasome regulatory particle: the first draft. Biochem. Soc. Trans. *38*, 6–13.

Pearce, M.J., Mintseris, J., Ferreyra, J., Gygi, S.P., and Darwin, K.H. (2008). Ubiquitin-like protein involved in the proteasome pathway of Mycobacterium tuberculosis. Science *322*, 1104–1107.

Peth, A., Besche, H.C., and Goldberg, A.L. (2009). Ubiquitinated proteins activate the proteasome by binding to Usp14/Ubp6, which causes 20S gate opening. Mol. Cell *36*, 794–804.

Pickart, C.M., and Cohen, R.E. (2004). Proteasomes and their kin: proteases in the machine age. Nat. Rev. Mol. Cell Biol. *5*, 177–187.

Prakash, S., Tian, L., Ratliff, K.S., Lehotzky, R.E., and Matouschek, A. (2004). An unstructured initiation site is required for efficient proteasome-mediated degradation. Nat. Struct. Mol. Biol. *11*, 830–837.

Prakash, S., Inobe, T., Hatch, A.J., and Matouschek, A. (2009). Substrate selection by the proteasome during degradation of protein complexes. Nat. Chem. Biol. *5*, 29–36.

Rabl, J., Smith, D.M., Yu, Y., Chang, S.C., Goldberg, A.L., and Cheng, Y. (2008). Mechanism of gate opening in the 20S proteasome by the proteasomal ATPases. Mol. Cell *30*, 360–368.

Rape, M., and Jentsch, S. (2004). Productive RUPture: activation of transcription factors by proteasomal processing. Biochim. Biophys. Acta *1695*, 209–213.

Rechsteiner, M., and Hill, C.P. (2005). Mobilizing the proteolytic machine: cell biological roles of proteasome activators and inhibitors. Trends Cell Biol. *15*, 27–33.

Religa, T.L., Sprangers, R., and Kay, L.E. (2010). Dynamic regulation of archaeal proteasome gate opening as studied by TROSY NMR. Science *328*, 98–102.

Rosenzweig, R., Osmulski, P.A., Gaczynska, M., and Glickman, M.H. (2008). The central unit within the 19S regulatory particle of the proteasome. Nat. Struct. Mol. Biol. *15*, 573–580.

Ruschak, A.M., Religa, T.L., Breuer, S., Witt, S., and Kay, L.E. (2010). The proteasome antechamber maintains substrates in an unfolded state. Nature *467*, 868–871.

Sadre-Bazzaz, K., Whitby, F.G., Robinson, H., Formosa, T., and Hill, C.P. (2010). Structure of a Blm10 complex reveals common mechanisms for proteasome binding and gate opening. Mol. Cell *37*, 728–735.

Schmidt, M., Haas, W., Crosas, B., Santamaria, P.G., Gygi, S.P., Walz, T., and Finley, D. (2005). The HEAT repeat protein Blm10 regulates the yeast proteasome by capping the core particle. Nat. Struct. Mol. Biol. *12*, 294–303.

Seemuller, E., Lupas, A., Stock, D., Lowe, J., Huber, R., and Baumeister, W. (1995). Proteasome from Thermoplasma acidophilum: a threonine protease. Science *268*, 579–582.

Shibatani, T., Carlson, E.J., Larabee, F., McCormack, A.L., Fruh, K., and Skach, W.R. (2006). Global organization and function of mammalian cytosolic proteasome pools: implications for PA28 and 19S regulatory complexes. Mol. Biol. Cell *17*, 4962–4971.

Smith, D.M., Kafri, G., Cheng, Y., Ng, D., Walz, T., and Goldberg, A.L. (2005). ATP binding to PAN or the 26S ATPases causes association with the 20S proteasome, gate opening, and translocation of unfolded proteins. Mol. Cell *20*, 687–698.

Smith, D.M., Chang, S.C., Park, S., Finley, D., Cheng, Y., and Goldberg, A.L. (2007). Docking of the proteasomal ATPases' carboxyl termini in the 20S proteasome's alpha ring opens the gate for substrate entry. Mol. Cell *27*, 731–744.

Sousa, M.C., Trame, C.B., Tsuruta, H., Wilbanks, S.M., Reddy, V.S., and McKay, D.B. (2000). Crystal and solution structures of an HslUV protease-chaperone complex. Cell *103*, 633–643.

Stadtmueller, B.M., Ferrell, K., Whitby, F.G., Heroux, A., Robinson, H., Myszka, D.G., and Hill, C.P. (2010). Structural models for interactions between the 20S proteasome and its PAN/19S activators. J. Biol. Chem. *285*, 13–17.

Striebel, F., Hunkeler, M., Summer, H., and Weber-Ban, E. (2010). The mycobacterial Mpa-proteasome unfolds and degrades pupylated substrates by engaging Pup's N-terminus. EMBO J. *29*, 1262–1271.

Suzuki, R., Moriishi, K., Fukuda, K., Shirakura, M., Ishii, K., Shoji, I., Wakita, T., Miyamura, T., Matsuura, Y., and Suzuki, T. (2009). Proteasomal turnover of hepatitis C virus core protein is regulated by two distinct mechanisms:

a ubiquitin-dependent mechanism and a ubiquitin-independent but PA28-gamma-dependent mechanism. J. Virol. *83*, 2389–2392.

Thomsen, N.D., and Berger, J.M. (2009). Running in reverse: the structural basis for translocation polarity in hexameric helicases. Cell *139*, 523–534.

Tian, L., Holmgren, R.A., and Matouschek, A. (2005). A conserved processing mechanism regulates the activity of transcription factors Cubitus interruptus and NF-kappaB. Nat. Struct. Mol. Biol. *12*, 1045–1053.

Tomko, R.J., Jr., Funakoshi, M., Schneider, K., Wang, J., and Hochstrasser, M. (2010). Heterohexameric ring arrangement of the eukaryotic proteasomal ATPases: implications for proteasome structure and assembly. Mol. Cell *38*, 393–403.

Unno, M., Mizushima, T., Morimoto, Y., Tomisugi, Y., Tanaka, K., Yasuoka, N., and Tsukihara, T. (2002). The structure of the mammalian 20S proteasome at 2.75 Å resolution. Structure *10*, 609–618.

Ustrell, V., Hoffman, L., Pratt, G., and Rechsteiner, M. (2002). PA200, a nuclear proteasome activator involved in DNA repair. EMBO J. *21*, 3516–3525.

Verma, R., Aravind, L., Oania, R., McDonald, W.H., Yates, J.R., 3rd, Koonin, E.V., and Deshaies, R.J. (2002). Role of Rpn11 metalloprotease in deubiquitination and degradation by the 26S proteasome. Science *298*, 611–615.

Walters, K.J., Lech, P.J., Goh, A.M., Wang, Q., and Howley, P.M. (2003). DNA-repair protein hHR23a alters its protein structure upon binding proteasomal subunit S5a. Proc. Natl. Acad. Sci. USA *100*, 12694–12699.

Wang, T., Li, H., Lin, G., Tang, C., Li, D., Nathan, C., and Darwin, K.H. (2009). Structural insights on the Mycobacterium tuberculosis proteasomal ATPase Mpa. Structure *17*, 1377–1385.

Wang, T., Darwin, K.H., and Li, H. (2010). Binding-induced folding of prokaryotic ubiquitin-like protein on the Mycobacterium proteasomal ATPase targets substrates for degradation. Nat. Struct. Mol. Biol. *17*, 1352–1357.

Wenzel, T., and Baumeister, W. (1995). Conformational constraints in protein degradation by the 20S proteasome. Nat. Struct. Biol. *2*, 199–204.

Whitby, F.G., Masters, E.I., Kramer, L., Knowlton, J.R., Yao, Y., Wang, C.C., and Hill, C.P. (2000). Structural basis for the activation of 20S proteasomes by 11S regulators. Nature *408*, 115–120.

Xu, P., Duong, D.M., Seyfried, N.T., Cheng, D., Xie, Y., Robert, J., Rush, J., Hochstrasser, M., Finley, D., and Peng, J. (2009). Quantitative proteomics reveals the function of unconventional ubiquitin chains in proteasomal degradation. Cell *137*, 133–145.

Yao, T., and Cohen, R.E. (2002). A cryptic protease couples deubiquitination and degradation by the proteasome. Nature *419*, 403–407.

Yao, T., Song, L., Xu, W., DeMartino, G.N., Florens, L., Swanson, S.K., Washburn, M.P., Conaway, R.C., Conaway, J.W., and Cohen, R.E. (2006). Proteasome recruitment and activation of the Uch37 deubiquitinating enzyme by Adrm1. Nat. Cell Biol. *8*, 994–1002.

Yu, Y., Smith, D.M., Kim, H.M., Rodriguez, V., Goldberg, A.L., and Cheng, Y. (2010). Interactions of PAN's C-termini with archaeal 20S proteasome and implications for the eukaryotic proteasome-ATPase interactions. EMBO J. *29*, 692–702.

Zhang, Z., Clawson, A., Realini, C., Jensen, C.C., Knowlton, J.R., Hill, C.P., and Rechsteiner, M. (1998). Identification of an activation region in the proteasome activator REGalpha. Proc. Natl. Acad. Sci. USA *95*, 2807–2811.

Zhang, F., Hu, M., Tian, G., Zhang, P., Finley, D., Jeffrey, P.D., and Shi, Y. (2009a). Structural insights into the regulatory particle of the proteasome from Methanocaldococcus jannaschii. Mol. Cell *34*, 473–484.

Zhang, F., Wu, Z., Zhang, P., Tian, G., Finley, D., and Shi, Y. (2009b). Mechanism of substrate unfolding and translocation by the regulatory particle of the proteasome from Methanocaldococcus jannaschii. Mol. Cell *34*, 485–496.